Estimation of proliferative potentiality of central neurocytoma: correlational analysis of minimum ADC and maximum SUV with MIB-1 labeling index.

AUTHOR(S):

Sakamoto, Ryo; Okada, Tomohisa; Kanagaki, Mitsunori; Yamamoto, Akira; Fushimi, Yasutaka; Kakigi, Takahide; Arakawa, Yoshiki; Takahashi, Jun C; Mikami, Yoshiki; Togashi, Kaori

CITATION:

Sakamoto, Ryo ...[et al]. Estimation of proliferative potentiality of central neurocytoma: correlational analysis of minimum ADC and maximum SUV with MIB-1 labeling index.. Acta radiologica 2014, 56(1): 114-120

ISSUE DATE:

2014-01-29

URL:

http://hdl.handle.net/2433/198568

Estimation of Proliferative Potentiality of Central Neurocytoma: Correlational Analysis of minimum ADC and maximum SUV with MIB-1 Labeling Index

Ryo Sakamoto, MD[1)], Tomohisa Okada, MD, PhD[1)*], Mitsunori Kanagaki, MD, PhD[1)], Akira Yamamoto, MD, PhD[1)], Yasutaka Fushimi, MD, PhD[1)], Takahide Kakigi, MD[1)], Yoshiki Arakawa, MD, PhD[2)], Jun C. Takahashi, MD, PhD[2)], Yoshiki Mikami, MD, PhD[3)], Kaori Togashi, MD, PhD[1)]

[1)] Department of Diagnostic Imaging and Nuclear Medicine, [2)] Department of Neurosurgery, and [3)] Department of Clinical Pathology, Kyoto University Graduate School of Medicine, Kyoto, Japan.

Type of the article: Original Research

Abstract

Background: Central neurocytoma was initially believed to be benign tumor type, although atypical cases with more aggressive behavior have been reported. Preoperative estimation for proliferating activity of central neurocytoma is one of the most important considerations for determining tumor management.

Purpose: To investigate predictive values of image characteristics and quantitative measurements of minimum apparent diffusion coefficient (ADCmin) and maximum standardized uptake value (SUVmax) for proliferative activity of central neurocytoma measured by MIB-1 labeling index (LI).

Material and Methods: Twelve cases of central neurocytoma including one recurrence from January 2001 to December 2011 were included. Preoperative scans were conducted in eleven, nine and five patients for computed tomography (CT), diffusion-weighted imaging (DWI) and fluorine-18-fluorodeoxyglucose positron emission tomography (FDG-PET), respectively, and ADCmin and SUVmax of the tumors were measured. Image characteristics were investigated using CT, T2WI and contrast-enhanced T1WI, and their differences were examined using the Fisher's exact test between cases with MIB-1 LI below and above 2%, which is recognized as typical and atypical central neurocytoma, respectively. Correlational analysis was conducted for ADCmin and SUVmax with MIB-1 LI. A P value < .05 was considered significant.

Results: Morphological appearances had large variety, and there was no significant correlation with MIB-1 LI except a tendency that strong enhancement was observed in central neurocytomas with

higher MIB-1 LI (P = 0.061). High linearity with MIB-1 LI was observed in ADCmin and SUVmax (r = -0.91 and 0.74, respectively), but only ADCmin was statistically significant (P = 0.0006).

Conclusion: Central neurocytoma had a wide variety of image appearance, and assessment of proliferative potential was considered difficult only by morphological aspects. ADCmin was recognized as a potential marker for differentiation of atypical central neurocytomas from the typical ones.

Key Words:

central neurocytoma; central nerve system (CNS); brain; MR-Diffusion; positron emission tomography (PET)

Introduction

Central neurocytoma is a rare low grade tumor of the central nervous system, which was first described by Hassoun et al. in 1982 (1). It is composed of uniform round cells with neuronal differentiation constituting approximately 0.25 to 0.5% of all intracranial tumors. It occurs typically in young adults and is located in the lateral or third ventricle around the foramen of Monro (2). Clinical course of the central neurocytoma was initially believed to be benign, however, more aggressive behavior including rapid tumor progression, recurrence, extra-ventricular extension and craniospinal dissemination has been described (3, 4). The term atypical central neurocytoma has been proposed for an aggressive variant of the central neurocytoma, which is classified if MIB-1 (Immunotech, Marseilles, France) labeling index (LI), an index of cellular proliferation, is higher than 2% (5) or atypical histologic features of focal necrosis, vascular proliferation and increased mitotic activity are observed (6). MIB-1 is a monoclonal antibody to Ki-67 antigen that is a nuclear protein associated with cellular proliferation.

For patients with the atypical central neurocytoma, complete resection is the best treatment for better local control and survival (7). Therefore, preoperative estimation for proliferating activity of the central neurocytoma is one of the most important considerations for determining the appropriate surgical strategy. There are some reports discussing imaging features of the central neurocytoma. They reported varying degrees of contrast enhancement with or without cystic appearance and calcification of tumors (8, 9), but mainly focused on differentiating neurocytomas

from other intraventricular tumors, and relationship between proliferative potential and morphological image findings has not been clarified.

As quantitative imaging marker of malignancy, diffusion weighted imaging (DWI) provides further physiologic information as apparent diffusion coefficient (ADC), which is helpful in grading brain tumors (10, 11) including central neurocytoma (12). ADC correlates with tumor cellularity, prognosis and MIB-1 LI in gliomas (13-15). Other than MRI, standardized uptake value (SUV) measured by ^{18}F-fluorodeoxyglucose-positron emission tomography (FDG-PET) reflects increased glucose metabolism and correlates with histological grade of gliomas (16). Mineura *et al.* reported rapid regrowth of central neurocytoma that had increased cerebral metabolic rate of glucose (17). Ohtani et al. reported a case of central neurocytoma with intense FDG uptake, which had a high MIB-1 LI and atypical pathological features (18). These cases indicate that SUV may also predict the proliferation potential of the central neurocytoma. However, preoperative estimation of the proliferative activity of the central neurocytoma has not been conducted.

Therefore in this study, we investigated if image characteristics and quantitative values of ADC and SUV could distinguish central neurocytomas with MIB-1 LI higher than 2% from those with lower values.

Material and Methods

This study was approved by institutional review board, and informed consent was waived, because

retrospective analysis was conducted.

Patients

Eleven patients from January 2001 to December 2011 at our institute were enrolled. Inclusion criteria was pathological confirmation of central neurocytoma and presence of preoperative imaging studies (CT, MRI and FDG-PET). There was one recurrent case at 3 years after partial tumor resection (patient 4 in Table 1). This case was enrolled as patient 4', and images just before secondary operation were also analyzed.

CT imaging

CT images were obtained parallel to the orbitomeatal line. Resolutions of all CT images were 0.4 × 0.4 × 7 - 8 mm.

MR imaging

MR scans were conducted with 1.5T scanners for 6 patients (patients 1, 3, 4, 4' and 6 with MAGNETOM Symphony, Siemens Medical Systems, Erlangen, Germany; patients 2 and 5 with Signa Genesis, GE Healthcare, Milwaukee, WI, USA) and 3T scanners for 5 patients (patients 7, 8 and 9 with MAGNETOM Trio; patients 10 and 11 with MAGNETOM Skyra, Siemens Medical Systems, Erlangen, Germany). In addition to conventional axial T1WI (TR/TE = 450 - 616/8.1 - 12

ms) and T2WI (TR/TE = 3180 - 7960/93 - 130 ms), contrast-enhanced axial T1WI were acquired after administration of the Gadolinium contrast agent (0.1 mmol/kg) in 11 cases. DWI was acquired in 9 cases with in-plane resolution = 0.69 - 1.38 mm and slice thickness/spacing = 3 - 5/1 - 1.5 mm using a single-shot echo-planar sequence with motion-probing gradients (b = 0, 1000 s/mm^2) applied in 3 orthogonal directions, and ADC map was calculated.

PET imaging

FDG-PET scans were conducted, using a PET scanner for 1 patient and a PET/CT scanner for 4 patients (patient 4' with Advance; patients 8 - 11 with Discovery ST Elite, GE Healthcare, Waukesha, WI, USA). Patients fasted for at least 4 hours prior to the scans. After intravenous administration of 4 MBq/kg of FDG, patients rested in a waiting room for 30 minutes. Emission scans of the brain were conducted for 15 minutes. Resolutions were 2.0 mm × 2.0 mm × 4.25 mm (35 slices) and 2.0 mm × 2.0 mm ×3.27 mm (47 slices), respectively for the scanners.

Image analysis

Appearance of the tumors was reviewed with regard to location, size, calcification on CT image (present/absent: if present, distribution = diffuse or patchy; density = faint or dense), cystic components on T2WI (distribution = diffuse or partial; uniformity = uniform or non-uniform; size = small or large) and degree of enhancement on contrast-enhanced T1WI (degree = none to slight or

moderate to marked, homogeneity = homogeneous or heterogeneous), and categorized by two board-certified neuroradiologists in consensus (R.S. and T.K., both had experience in diagnostic imaging for 8 years).

For quantitative analysis, regions of interest (ROIs) were defined independently by two neuroradiologists (RS and TK) at different areas (2 to 3 areas) within the tumors of the ADC maps and SUV images (ROI size: 50 - 361 mm^2 and 114 - 513 mm^2, respectively) using a free software (MRIcro, http://www.mccauslandcenter.sc.edu/mricro/, provided by Chris Rorden, Neuropsychology Lab, Columbia SC, USA). Cares were paid to exclude macroscopic calcifications and cysts on each modality referencing to CT image and T2WI. From the values of the ROIs, minimum ADC (ADCmin) and maximum SUV (SUVmax) were extracted.

Proliferative activity

Proliferative activity was measured as MIB-1 LI in formalin-fixed paraffin embedded pathological specimens with immuno-histochemical staining using MIB-1 monoclonal antibody. Areas with highest number of positive nuclei were identified, and a minimum of 1,000 cells were counted in each tissue section (Y.M. a board-certified pathologist majoring in surgical neuropathology). MIB-1 LI was defined as the percentage of tumor cells which stained positively for Ki-67 nuclear antigen.

Statistical analysis

Intra-class correlation coefficients (ICCs) for measured values in the ROIs were evaluated. Image characteristics were compared between two tumor groups with MIB-1 LI lower to equal to or higher than 2% using Fisher's exact test. ADCmin and SUVmax values were assessed by linear regression analyses with values of MIB-1 LI. ROC analysis was conducted to investigate differential capability of atypical central neurocytomas from typical ones, when there was a significant correlation. A *P* value less than 0.05 was considered statistically significant. Statistical analyses were conducted using commercially available software (MedCalc, version 12.4.0; MedCalc Software, Acacialaan 22, B-8400 Ostend, Belgium).

Results

Characteristics of the patients and tumor images are summarized in Table 1. All of the tumors were located in the lateral ventricle and had an attachment to the ventricular wall or septum pellucidum. CT scans showed calcifications of variable density and distribution. Almost all tumors had heterogeneous appearance with solid portion and cysts that were variable in number and size. MRI showed that most tumors were iso- to hypo-intense on T1WI and hyper-intense on T2WI. Contrast enhancement of tumors was homogenous or heterogeneous, and degree of enhancement was varied. Six tumors showed none to slight enhancement and 5 tumors had moderate to marked enhancement, and a tendency that strong enhancement was observed in tumors with higher MIB-1 LI ($P = 0.061$). There was no significant difference in other image characteristics. Fig. 1 shows representative case

images (patient 10) and Fig. 2 visually summarizes image characteristics.

The quantitative values of MIB-1 LI, ADCmin and SUVmax are listed in Table 2 and Fig. 3 shows DWI, ADC map and FDG-PET/CT images of a representative case. MIB-1 LI ranged from 0.09 to 5.62% (mean ± S.D.: 3.26 ± 1.88%). Four tumors had MIB-1 LI lower than 2%, and eight tumors had those higher than 2%. ICCs of the ROI analyses were 0.97 for ADCmin and 0.96 for SUVmax, which means excellent agreements. ADCmin values ranged from 0.23 to 1.05 × 10^{-3} mm^2/s, and significant linear correlation was observed with MIB-1 LI (r = -0.91, P = 0.0006). ROC analysis showed that the atypical central neurocytoma could be differentiated from typical one with 100% sensitivity (95% C.I.: 47.8 - 100.0%) and 100% specificity (39.8 - 100.0%), when the threshold value of ADCmin was set at 0.55 × 10^{-3} mm^2/s (P < 0.0001). The SUVmax ranged from 3.35 to 7.61. The values had high correlation with MIB-1 LI (r = 0.74), but it was not significant (P = 0.15). These linear relationships are presented in Fig. 4.

Discussion

Although the central neurocytoma has been considered indolent, there are some cases that showed aggressive biologic behavior including postoperative rapid regrowth (19, 20). Among many pathologic features, elevated MIB-1 LI correlates with an increased recurrence rate and poor outcome (5, 21) and is thought to be a reliable immune-histopathologic marker (5). No significant correlation was found between other histopathologic characteristics and clinical outcome (22, 23). In

this study, large variety was observed in calcification and cystic changes, and only strong enhancement suggested increased proliferative potential as in the former case reports (24, 25).

Our result of MIB-1 LI is congruent with the previous reports ranging less than 0.1 to 11.2% (5, 21, 23). There was a significant negative linear correlation between MIB-1 LI and ADCmin as was in other type of brain tumors (13). ADC value has an inverse relation with tumor grades (10, 26), and poor survival was reported in malignant glial tumors with lower ADCmin (14, 27). Our result indicates that lower ADCmin reflects malignant potential of the central neurocytoma. In case patient 4, the tumor had a high MIB-1 LI (5.62%) with a lower ADCmin (0.45×10^{-3} mm^2/s) than the proposed threshold. After partial resection, the tumor regrew gradually in three-year follow up (patient 4'). The recurrent tumor showed a high SUVmax (7.61) before second operation, and the pathologic specimen revealed that tumor maintained high proliferative activity (MIB-1 LI = 4.68%).

Increased glucose metabolism indicates higher proliferative activity of the brain tumor (28). Our study presented high linearity between SUVmax and MIB-1 LI. This result may help to facilitate the usage of FDG-PET examinations in the central neurocytoma as in a previous case report which demonstrated that a central neurocytoma with higher FDG uptake showed an increased proliferative index associated with atypical histological features (18).

There are several limitations in this study. First, the number of cases is small. However, it is considered inevitable, because the central neurocytoma is relatively rare. Because of this rarity, the enrollment period was very long. Therefore second, not all image examinations were available, and

different scanners and parameters were used particularly in MR Imaging.

In conclusion, central neurocytomas had a variety of image appearances, and there was no significant correlation with MIB-1 LI except a tendency that central neurocytomas with higher MIB-1 LI demonstrated stronger enhancement. Assessment of proliferative potential would be difficult if only morphological aspects are considered. ADCmin showed significant linear correlation with MIB-1 LI, and SUVmax had the same tendency. Both quantitative imaging values of ADCmin and SUVmax, especially for ADCmin, are considered as potential markers for predicting high MIB-1 LI of central neurocytoma.

Funding

This research received no specific grant from any funding agency in the public, commercial, or not-for-profit sectors.

References

1 Hassoun J, Gambarelli D, Grisoli F, *et al.* Central neurocytoma. An electron-microscopic study of two cases. Acta Neuropathol 1982;**56**:151-156.

2 Hassoun J, Soylemezoglu F, Gambarelli D, *et al.* Central neurocytoma: a synopsis of clinical and histological features. Brain Pathol 1993;**3**:297-306.

3 Bertalanffy A, Roessler K, Koperek O, *et al.* Recurrent central neurocytomas. Cancer

2005;**104**:135-142.

4 Takao H, Nakagawa K, Ohtomo K. Central neurocytoma with craniospinal dissemination. J Neurooncol 2003;**61**:255-259.

5 Soylemezoglu F, Scheithauer BW, Esteve J, *et al.* Atypical central neurocytoma. J Neuropathol Exp Neurol 1997;**56**:551-556.

6 Brat DJ, Scheithauer BW, Eberhart CG, *et al.* Extraventricular neurocytomas: pathologic features and clinical outcome. Am J Surg Pathol 2001;**25**:1252-1260.

7 Rades D, Fehlauer F, Schild SE. Treatment of atypical neurocytomas. Cancer 2004;**100**:814-817.

8 Zhang B, Luo B, Zhang Z, *et al.* Central neurocytoma: a clinicopathological and neuroradiological study. Neuroradiology 2004;**46**:888-895.

9 Chen H, Zhou R, Liu J, *et al.* Central neurocytoma. J Clin Neurosci 2012;**19**:849-853.

10 Kono K, Inoue Y, Nakayama K, *et al.* The role of diffusion-weighted imaging in patients with brain tumors. Am J Neuroradiol 2001;**22**:1081-1088.

11 Bulakbasi N, Guvenc I, Onguru O, *et al.* The added value of the apparent diffusion coefficient calculation to magnetic resonance imaging in the differentiation and grading of malignant brain tumors. J Comput Assist Tomogr 2004;**28**:735-746.

12 Kocaoglu M, Ors F, Bulakbasi N, *et al.* Central neurocytoma: proton MR spectroscopy and diffusion weighted MR imaging findings. Magn Reson Imaging 2009;**27**:434-440.

13 Higano S, Yun X, Kumabe T, *et al.* Malignant astrocytic tumors: clinical importance of apparent

diffusion coefficient in prediction of grade and prognosis. Radiology 2006;**241**:839-846.

14 Zulfiqar M, Yousem DM, Lai H. ADC values and prognosis of malignant astrocytomas: does lower ADC predict a worse prognosis independent of grade of tumor?--a meta-analysis. Am J Roentgenol 2013;**200**:624-629.

15 Le Bihan D. Apparent diffusion coefficient and beyond: what diffusion MR imaging can tell us about tissue structure. Radiology 2013;**268**:318-322.

16 Padma MV, Said S, Jacobs M, *et al.* Prediction of pathology and survival by FDG PET in gliomas. J Neurooncol 2003;**64**:227-237.

17 Mineura K, Sasajima T, Itoh Y, *et al.* Blood flow and metabolism of central neurocytoma: a positron emission tomography study. Cancer 1995;**76**:1224-1232.

18 Ohtani T, Takahashi A, Honda F, *et al.* Central neurocytoma with unusually intense FDG uptake: case report. Ann Nucl Med 2001;**15**:161-165.

19 Warmuth-Metz M, Klein R, Sorensen N, *et al.* Central neurocytoma of the fourth ventricle. Case report. J Neurosurg 1999;**91**:506-509.

20 Wharton SB, Antoun NM, Macfarlane R, *et al.* The natural history of a recurrent central neurocytoma-like tumor. Clin Neuropathol 1998;**17**:136-140.

21 Mackenzie IR. Central neurocytoma: histologic atypia, proliferation potential, and clinical outcome. Cancer 1999;**85**:1606-1610.

22 Vasiljevic A, Francois P, Loundou A, *et al.* Prognostic factors in central neurocytomas: a multicenter

study of 71 cases. Am J Surg Pathol 2012;**36**:220-227.

23 Ashkan K, Casey AT, D'Arrigo C*, et al.* Benign central neurocytoma. Cancer 2000;**89**:1111-1120.

24 Ogawa Y, Sugawara T, Seki H*, et al.* Central neurocytomas with MIB-1 labeling index over 10% showing rapid tumor growth and dissemination. J Neurooncol 2006;**79**:211-216.

25 Kuchiki H, Kayama T, Sakurada K*, et al.* Two cases of atypical central neurocytomas. Brain Tumor Pathol 2002;**19**:105-110.

26 Lee EJ, Lee SK, Agid R*, et al.* Preoperative grading of presumptive low-grade astrocytomas on MR imaging: diagnostic value of minimum apparent diffusion coefficient. Am J Neuroradiol 2008;**29**:1872-1877.

27 Yamasaki F, Sugiyama K, Ohtaki M*, et al.* Glioblastoma treated with postoperative radio-chemotherapy: prognostic value of apparent diffusion coefficient at MR imaging. Eur J Radiol 2010;**73**:532-537.

28 Kruer MC, Kaplan AM, Etzl MM, Jr.*, et al.* The value of positron emission tomography and proliferation index in predicting progression in low-grade astrocytomas of childhood. J Neurooncol 2009;**95**:239-245.

Tables.

Table 1. Characteristics of the patients and tumor images

Patient No.	Sex / Age (yr)	Location	Size (mm)	Calcification on CT distribution / density	Cystic appearance on T2WI distribution / uniformity / size	Enhancement on Gd-T1WI degree / homogeneity
1	M/31	LtLV~3V	54 × 43	diffuse / dense	diffuse / non-uniform / large	none / n.a.
2	F/34	RtLV	61 × 39	patchy / dense	diffuse / non-uniform / large	n.a. / n.a.
3	M/35	RtLV	39 × 18	none	diffuse / uniform / small	none / n.a.
4	F/21	RtLV	42 × 37	patchy / faint	partial / non-uniform / small	marked / heterogeneous
4’	F/24	RtLV	27 × 20	none	partial / uniform / small	marked / homogeneous
5	F/38	LtLV	39 × 25	patchy / dense	diffuse / non-uniform / large	slight / homogeneous
6	F/54	LtLV	63 × 44	none	partial / non-uniform / large	marked / homogeneous
7	M/22	LtLV~3V	59 × 40	patchy / faint	diffuse / non-uniform / small	none / n.a.
8	M/28	LtLV	27 × 19	none	partial / uniform / small	moderate / heterogeneous
9	M/34	RtLV	29 × 25	patchy / faint	diffuse / non-uniform / large	none / n.a.
10	M/34	LtLV	21 × 17	none	diffuse / uniform / small	moderate / homogeneous
11	M/26	LtLV	15 × 13	none	partial / uniform / small	none / n.a.

LtLV: left lateral ventricle, RtLV: right lateral ventricle, 3V: third ventricle, n.a.: not applicable, Gd-T1WI: Gadolinium-enhanced T1WI

Table 2. MIB-1 LI, ADCmin and SUVmax of the central neurocytomas

Patient No.	MIB-1 LI (%)	ADCmin (10^{-3} mm^2/s)	SUVmax
1	0.77	0.92	n.a.
2	5.42	n.a.	n.a.
3	0.09	0.95	n.a.
4	5.62	0.45	n.a.
4’	4.68	n.a.	7.61
5	1.15	1.05	n.a.
6	3.03	n.a.	n.a.
7	1.98	0.73	n.a.
8	3.95	0.45	5.60
9	3.28	0.55	3.35
10	4.12	0.26	4.55
11	5.03	0.23	5.61

MIB-1 LI: MIB-1 labeling index, ADCmin: minimum value of ADC in the tumor ROI, SUVmax: maximum of SUV, n.a.: not applicable

Figures.

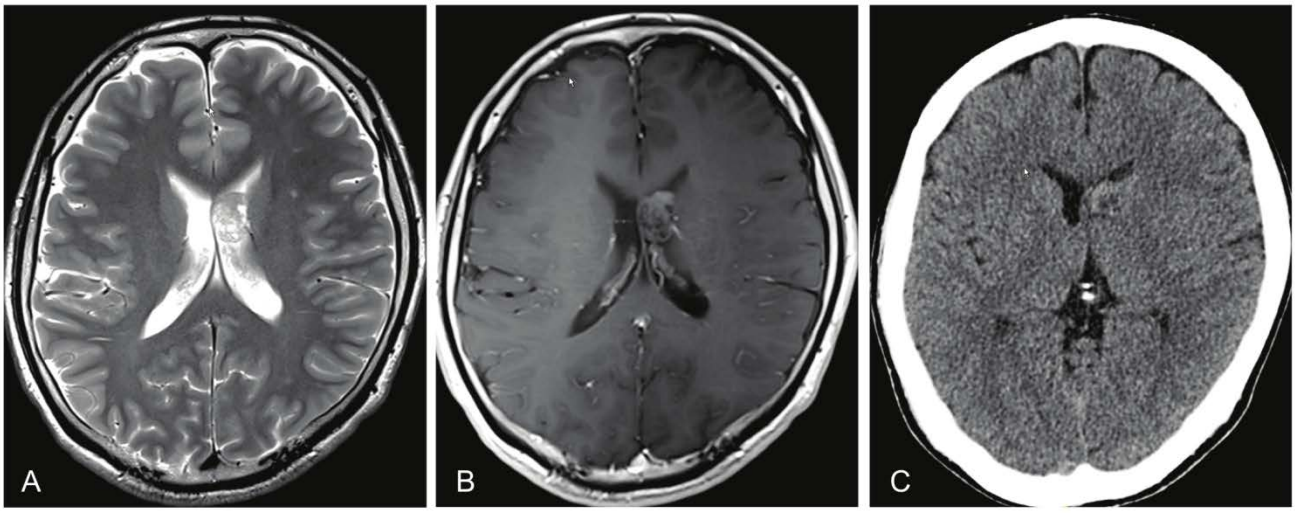

Figure 1. A representative case of a central neurocytoma located at the left lateral ventricle (patient 10). Diffusely distributed small cysts on T2WI (A) and moderately enhanced solid portion on contrast-enhanced T1WI (B) are noted. Calcification is not identified on CT (C).

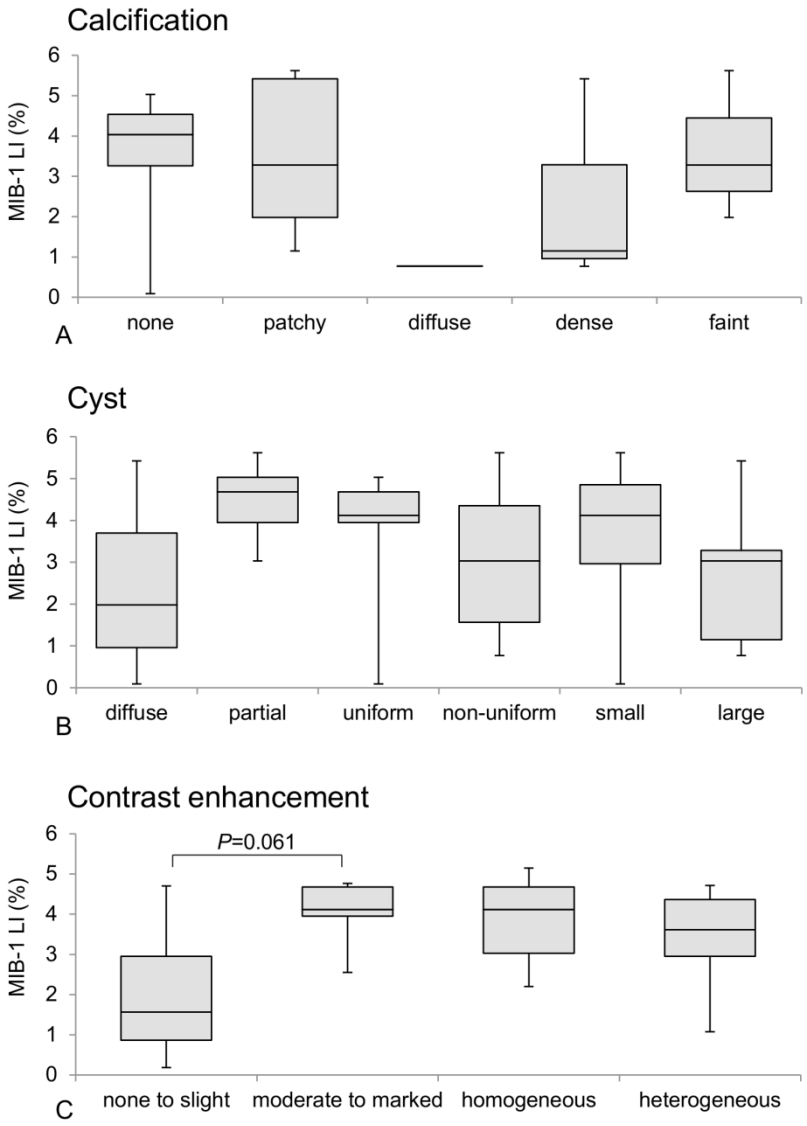

Figure 2. Box plots show the relationship of MIB-1 LI values with the following image characteristics: (A) calcification on CT (none or present, patchy or diffuse, and dense or faint), (B) cysts on T2WI (diffuse or partial, uniform or non-uniform, and small or large), and (C) contrast enhancement on T1WI (none to slight or moderate to marked, and homogeneous or heterogeneous). Image characteristics of tumors varies greatly and only the difference in contrast enhancement between none to slight and moderate to marked is marginally significant (P = 0.061) between tumors with MIB-1 LI lower or higher than 2% using Fisher's exact test.

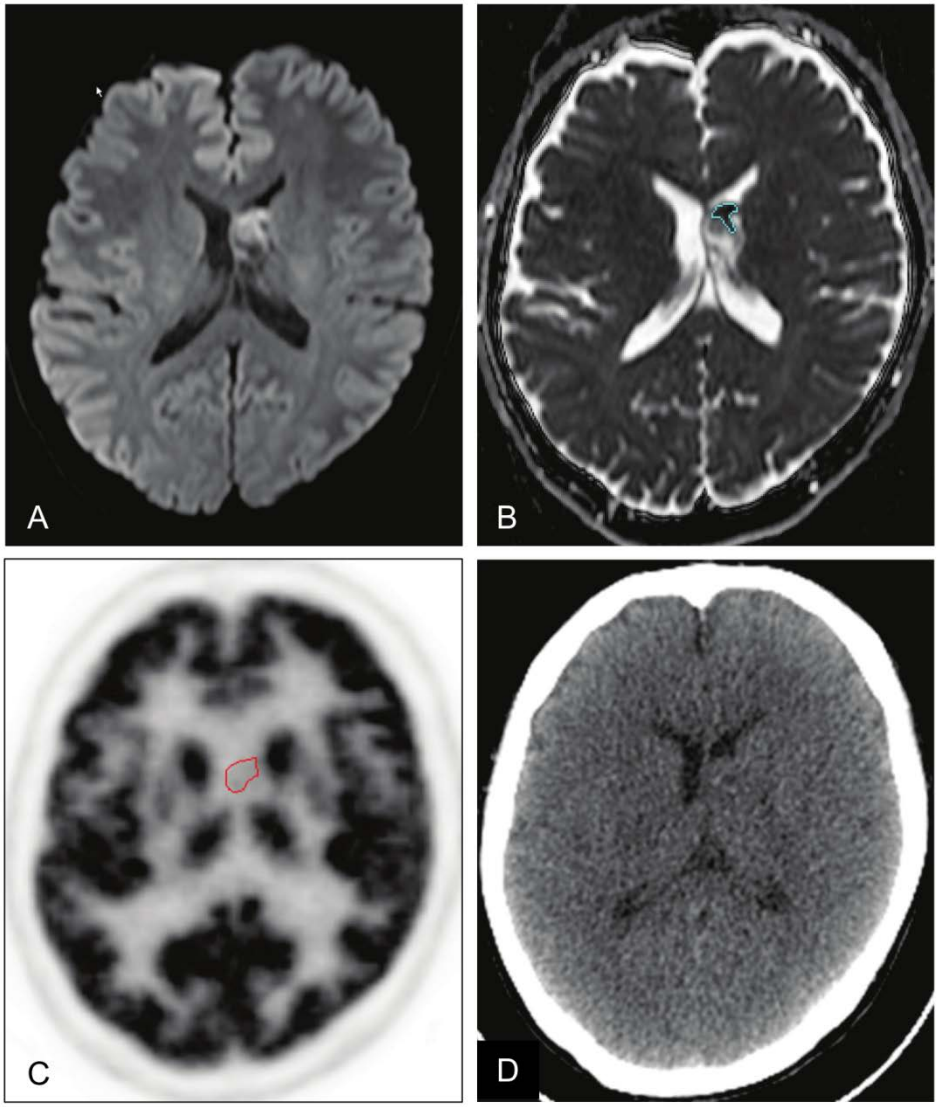

Figure 3. The solid portion of the tumor in the representative case shows high signal on DWI (A) and restricted diffusion on ADC map, where a ROI for ADCmin is drawn (B). A ROI for SUVmax is defined at the same location on FDG-PET (C), referring to simultaneously acquired CT image (D).

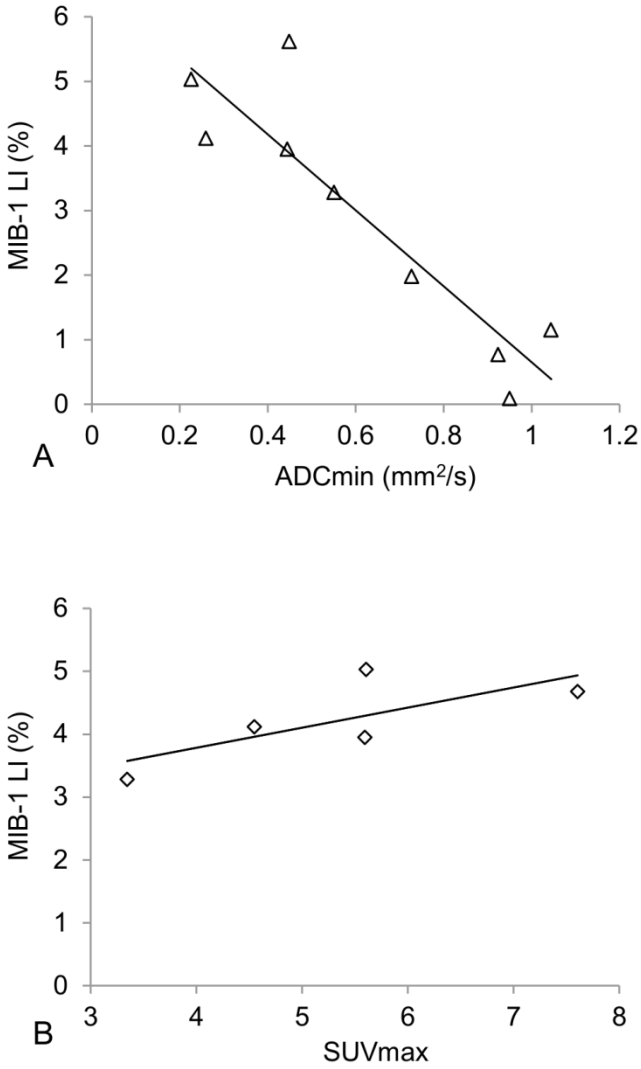

Figure 4. (A) Linear regression analyses shows significant negative correlation (r = -0.9) between ADCmin and MIB-1 LI (P = 0.0006). (B) There is high correlation between SUVmax and MIB-1 LI (r = 0.74), but it is not statistically significant (P = 0.15).